

Use of 3D scanning technique to determine tire deformation in static conditions

Weronika Ptak, Jaroslaw Czarnecki, Marek Brennensthul

Wroclaw University of Environmental and Life Sciences, Institute of Agricultural Engineering, Wroclaw, Poland

Abstract

This paper presents an innovative digital method to analyse agricultural tire profiles based on pictures. From this method, we can conclude that the tire deformation is caused by the changes in vertical load and inflation pressure. The first stage in this method is 3D-scanning; the vertical cross-section is created from the obtained picture of the tested tire. From this cross-section, the deflection of the tire can be determined. Then, the horizontal cross-section is created - this operation allows determining the tire's contact area at the highest vertical deformation. Obtained results can be useful to create the tire deformation characteristic. In turn, the contact pressure values can be determined (even through laboratory testing, without research in field conditions). The knowledge about contact pressure allows taking some actions to reduce soil compaction. In the description of the method, the radial tire was used, but the structure and equipment of the test bench allow the use of cross-ply tires with different dimensions.

Introduction

Nowadays, in farming production, the choice of appropriate technologies is a very important factor. Moreover, in the case of agricultural vehicles, the choice of technical-exploitation parameters of the tires is essential. Consequences of inadequate choice of these parameters can be reflected in excessive soil compaction; further, the soil environment can be exposed to severe disturbances (Ani *et al.*, 2018; Guimarães Júnnyor *et al.*, 2019; Keller and *et al.*, 2019). For this reason, information about phenomena in

the tire-surface system is required.

Recently, two main types of agricultural tires (with different internal structures) are available in the market. The first type consists of bias-ply tires that have greater mechanical strength - these tires are more resistant to damages, but are less flexible. The second type is composed of the radial tires - in this case, the flexibility is higher than in bias-ply tires, so the possibility of use of low inflation pressures is higher too (Lindemuth, 2006). Due to the farming practice, the appropriate total range of the inflation pressure is 0.8-2.0 bar. At the field operations, the inflation pressure should be in the range 0.8-1.2 bar, while at the transportation, inflation pressure can be higher (above 1.2 to 2.0 or even higher - in the case of tires with higher dimensions). It is related to different deformability - on the soft surfaces, a tire with low pressure can have a greater contact area than a tire with high pressure. In turn, it limits the sinkage of the tire - as a result, the compaction is lower. On the other hand, inflation pressure should be higher than in the field at the transportation because it can reduce rolling resistance. Manufacturers of the agricultural tires recommend specific inflation pressure values depending on tire dimensions, load, and velocity (Kowalski, 2006). These changeable parameters determine the deformation of the tire and, as a consequence, they affect the tire-surface area (Arvidsson and Keller, 2007; Diserens *et al.*, 2011; Taghavifar and Mardani, 2013).

Due to the different stiffness of tires, their action on surfaces will be changeable. For this reason, it is necessary to research tires in the aspect of flexibility (Misiewicz *et al.*, 2016; Anifantis *et al.*, 2020). In the same cases, the deflection is measured by sensors (Song *et al.* 2018), while in other research, more complex methods are used - for example, in (Anifantis *et al.*, 2020). However, it can be stated that the parameters of the tires (*i.e.*, sizes, design, internal structure) are so different that the determination of flexibility is a complex issue. For this reason, in literature, there are more publications about the impact of tires on surfaces.

Many authors use different methods to measure the tire-surface contact area and soil deformation resulting from wheels' static and dynamic effects (Błaszkiwicz, 1990; Wulfsohn and Upadhyaya, 1992). The simplest are based on tires footprints measurements (Grečenko, 1995). In general, based on mathematical and geometric models as well as on the elasticity theory, they determine the contact area using a rectangular coordinate system and elliptical estimation. By means of a profilometer, Jurga (2008) studied soil deformation, performing measurements of the rut formed by the passage of wheels. Diserens (2009) used a photometric method, taking pictures of the tire-soil contact surfaces and then analysing them in the Adobe Photoshop Elements software. Derafshpour *et al.* (2019) filmed the passage of a tire on glass covered with a special liquid to observe the change in the area of the tire contact with the surface using the technique of image processing. Kumar *et al.* (2018) used carbon paper between two sheets of white paper, placing them under a tire.

The latest methods to study changes in shape, dimensions, and

Correspondence: Weronika Ptak, Wroclaw University of Environmental and Life Sciences, Institute of Agricultural Engineering, 51-630, Wroclaw, Poland.

E-mail: weronika.ptak@upwr.edu.pl

Key words: Agricultural tire; 3D scanning; contact pressure; tire deformation.

Received for publication: 24 June 2021.

Accepted for publication: 2 December 2021.

© Copyright: the Author(s), 2022

Licensee PAGEPress, Italy

Journal of Agricultural Engineering 2022; LIII:1221

doi:10.4081/jae.2022.1221

This article is distributed under the terms of the Creative Commons Attribution Noncommercial License (by-nc 4.0) which permits any non-commercial use, distribution, and reproduction in any medium, provided the original author(s) and source are credited.

area include digital image analysis technology with 3D scanning. This method has been widely used, among others, in medicine, materials science, assembly lines, or the machine wear testing (Stawicki, 2018; Lazarević *et al.*, 2019; Alontseva *et al.*, 2020; Zhang *et al.*, 2020). For example, Farhadi *et al.* (2018) used a 3D scan to measure plaster of Paris moulds of tire footprints on the soil to study the volume of the rut, with its width and depth.

According to the literature, the studies of the wheel-surface contact are carried out by different methods, but only a small part of them allow spatial analysis already at the experiment stage. Moreover, only some of them allow immediate visualization of the spatial image of the tire (during the experiment). In these methods, individual analysis of each plane is realised; then the spatial picture is created. Whereas in these methods, a three-dimensional picture of tire profile is applied (during the experiment) - the individual analysis of separate planes is not needed. Most often, what is analysed is planes, which are used to create spatial models at a later stage. Therefore, it has become appropriate to develop a method that allows for quick spatial imagery of objects (wheel and surface interacting with each other). Based on such a spatial model, any number of planes, like tire cross-section or tire-soil contact surface, will be analysed. For these reasons, this paper aimed to present the innovative method of digital analysis of agricultural tires, especially to evaluate their deformation at different vertical loads and inflation pressures.

Materials and methods

The overall concept of the experiment was to develop a method of static tests of agricultural tires through digital analysis of the spatial image of their profile. In this way, applying various vertical loads and air pressure, it was possible to characterize tires in terms of their horizontal and vertical deformation and of their contact with the surface. Various vertical loads and air pressure in the tire were used as experimental factors. It was assumed that the first stage static tests would be carried out under laboratory conditions on a non-deformable surface - during this test, the tire footprint was created with no torque applied. The test bench allowed testing tires of different sizes and designs. The one used in the present experiment was the radial 500/50R17 tire, and its technical parameters are presented in Table 1.

Characteristics of the test bench

The design of the test bench made it possible to carry out tests on two types of surfaces: i) non-deformable surfaces - intended to predetermine the characteristics of the tire, mainly related to its deformability; such tests can be used as a model for further research; ii) deformable surfaces - intended to study the interaction of the tire with a particular surface. It will be possible to determine both the deformation of the tire and the surface. The surface material (*e.g.*, soil) will be placed in the so-called soil bathtub; iii) the present article sets out the principles of measuring and analysing the results for the non-deformable surface.

The research tools consist of two main parts: i) universal test bench for various static vertical load values, which was self-designed and made from standard elements of the steel. The only pieces from the market were the sensor (to measure vertical load) and the hydraulic jack; ii) a kit for creating and analysing a digital image of the tire profile.

With its outline presented in Figure 1A and its overall view in Figure 1B, the test bench allows applying various load values to

non-drive wheels of agricultural trailers, spreaders, or balers, *i.e.*, machinery causing soil compaction. In this experiment, only non-driving wheels were tested because the test bench was not fitted in the driving mechanism of the tire. The presented test bench is appropriate to static tests - their results will allow creating the characteristics of tire deformation. Moreover, the tests of non-driving wheels have practical justification because these tires can be exposed to the highest loads; the driving wheels in the tractors are sometimes equipped in systems to inflation pressure control, while the tires in trailers/balers/spreaders are not equipped in these systems. The design of the test bench is based on a vertical frame (3) made of steel closed profiles (Figure 1A). The tested tire (2) is mounted on a shaft with bearings, which in turn, is fixed to the inner frame (4). As a result of the use of linear steel guides, the inner frame can only move vertically, eliminating the risk of unintentional movement of the wheel.

The smooth change in the vertical load of the tire is achieved through a hydraulic cylinder (6) located between the main frame and the inner frame. The vertical load is measured using the TecSis dynamometer (5) with a measurement accuracy of 50 N and a measuring range of 0-100 kN. Therefore, the maximum vertical load that can be obtained with the hydraulic cylinder is 50 kN. This value is within the range of the vertical load of an agricultural machinery tire, often found in practice (Brennenstul, 2016). It is also in line with the maximum tire load capacity recommended by the manufacturer (described in the load index and in the catalogue data). The screw mechanisms (7) mounted at the top of the test bench are used to lock the position of the inner frame (4). The test bench allows the research of tires with a maximum external diameter of 1500 mm and a maximum width of 500 mm. Due to the recommendations of tires manufacturers and the ETRTO book, the values of the vertical loads for the tires with described dimensions do not exceed 4000-4500 kg. For this reason, the elements of the test bench (in the aspect of mechanical strength) were chosen to a maximum load of about 5000 kg. Therefore, the maximum capacity of the hydraulic jack was 4500 kg. Technical parameters of the tested bench are presented in Table 2.

Table 1. Technical parameters of the tested tire.

Parameter	500/50R17
Construction	Radial tire
External diameter (mm)	932
Profile width (mm)	500
Profile indicator (%)	50
Rim diameter (inch/mm)	17/432
Profile height (mm)	250
Load index (-)	146
Max load (kg)	3250

The kit for creating and analysing a digital tire profile image consists of a 3D scanner (SMARTTECH3D UNIVERSE, SMARTTECH3D, Poland, Warsaw, www.smarttech3d.com/), whose technical parameters are presented in Table 3. The scanner was connected to a laptop with dedicated Smarttech3D measure software, enabling continuous real-time data visualization.

Scanning process

The tests began with the installation of the wheel at the test bench, with the scanner placed on the ground. Scanning was carried out from 12 different positions around the tire to cover its different parts and contact with the surface. Before scanning, parameters such as tire air pressure and vertical load were preset. The load, *i.e.*, the force produced by the hydraulic cylinder, changed smoothly, and its values were available on the laptop. Once the required load value was reached, the inner frame was mechanically locked by means of the screw mechanism, eliminating the risk of inadvertently reducing the vertical load due to a drop in pressure in the hydraulic cylinder (*e.g.*, due to internal leaks). Because the tire was black, it was covered with anti-glare spray coating (with white matt surface) to achieve greater contrast so that the light of the scanner could more accurately record the scanned object.

Such procedure is used to scan dark objects - an alternative to coating is painting the object white. Since the scanner can only be used up to a specific volumetric size, larger objects are divided into parts to be scanned; then all those scans are combined using the scanner software. The result is a spatial image of the tire profile.

Before scanning, an ellipse was drawn around the test bench on the ground, with 12 marked points indicating where the scanner had to be positioned when scanning parts of the tire. The connection of the many scans was a native function of the scanning laser equipment. The ellipse with the scanner's location was developed based on previous tests - the distance between the scanner and tire was determined by measuring the volume of the scanner. Figure 2 shows the layout of the scanner locations to ensure that the full spatial image of the tire was obtained. These positions opposite the tread are closer to each other due to the different geometry of this

part of the tire, requiring more images to be taken. The optimal distance of the scanner (its working distance) was when three light beams emitted by the projector met, indicating the centre of the scanning volume. Figure 3 (left part) shows the scanning effect when the location points of the scanner were evenly spaced, with red colour indicating parts of the tire not captured by the scanning volume. This was due to the positions of the scanner, in general, angled with respect to the tire median plane. With the scanner positions opposite the thread closer to each other, it was possible to fill in the 'blank spaces'. The effects are highlighted in green in Figure 3 (right part), with the tire's shoulders clearly visible.

Table 2. Technical parameters of the tested bench.

Parameter	Value
Height (mm)	2100
Width (mm)	950
Length (mm)	700
Max external diameter of tested tire (mm)	1500
Max width of tested tire (mm)	500
Max displacement achievable by the hydraulic jack (mm)	320
Weight (without tire) (kg)	90

Table 3. Technical specification of 3D scanner.

Parameter	Description
Scanning technology	white structural light - LED
Measuring volume (x*y*z) (mm)	400×300×240
Distance between points (x*y) (mm)	0.156
Accuracy (mm)	0.08
Power consumption during measurement (W)	200
Weight (kg)	4.40
Working temperature (°C)	20+/-0.5

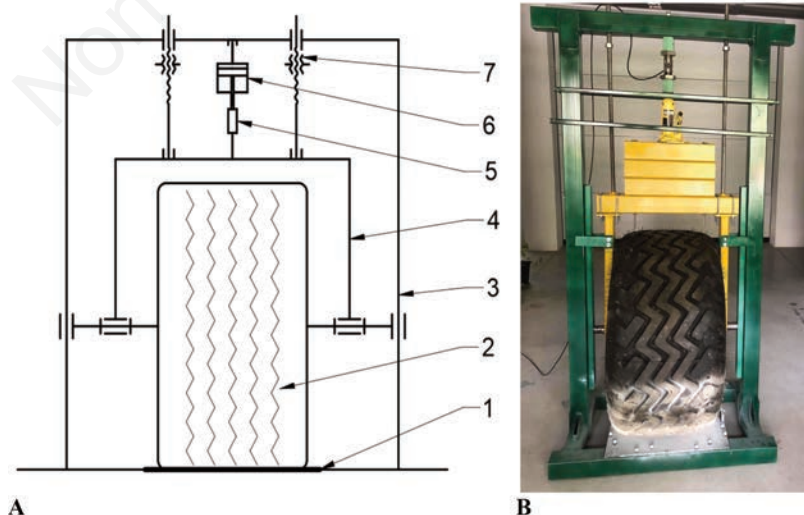


Figure 1. A) The outline of a test bench to study tires with different loads applied: 1- surface, 2- wheel with tire, 3- main frame, 4- inner frame, 5- dynamometer, 6- hydraulic cylinder, 7- screw mechanism for locking the position of the inner frame. B) Overall view of a test bench to study tires with different loads applied.

The scanner software allows filling blank spaces, but the two extreme edges of the tire tread need to be scanned to use it. The blank spaces could be caused by a lack of continuity of the picture created after scanning. It can negatively influence the created spatial picture of the tire. Therefore, it is better if the positions of the scanner are closer to each other. Based on previous tests, it was assumed that for a tire approximately 500 mm wide and approximately 900 mm in diameter, the optimum number of the positions would be 12. With fewer scanner locations, the scanning process would be faster, but the images obtained (particularly the tire tread) would not be sufficiently mapped. On the other hand, it would be too time-consuming to perform more scans, and the resulting tire image would not differ in accuracy compared to the number of scans finally taken. Of course, this method can also be used for tires with other external dimensions, but it is advisable to predetermine the number of the scanner positions beforehand.

The result of the combination of individual scans of different parts was a spatial image of the tire profile consisting of a point cloud (Figure 4A). This image allowed creating a mesh of triangles (Figure 4B) that was the basis for determining horizontal and ver-

tical sections of the tire profile. An essential element for scanning was the surface as a reference plane to help further analyse the image. The surface scan included a view of its front part (the surface was made up of a flat piece of sheet metal 4 mm thick).

The mesh of triangles was used to draw cross-sections, which were then exported to AutoCad 2019 (Auto-Desk), where detailed results were obtained from the analysis of tire deformation depending on vertical load and tire air pressure. First, the A-A vertical plane cross-section passing through the tire-surface contact was analysed (Figure 5). Based on this section, it was possible to determine both the vertical deformation of the profile (flattening) and the horizontal deformation (the tire sidewalls move away from each other). Horizontal section B-B was then analysed with a plane parallel to the surface, with its distance from the surface, or height (hp), at the largest horizontal deformation of the tire after the load was applied.

Based on the vertical section analysis (A-A, Figure 5), the width of the tire profile (b) and vertical deformation or flattening (h) were read from the graphics program. An example of a vertical section is presented in Figure 6A.

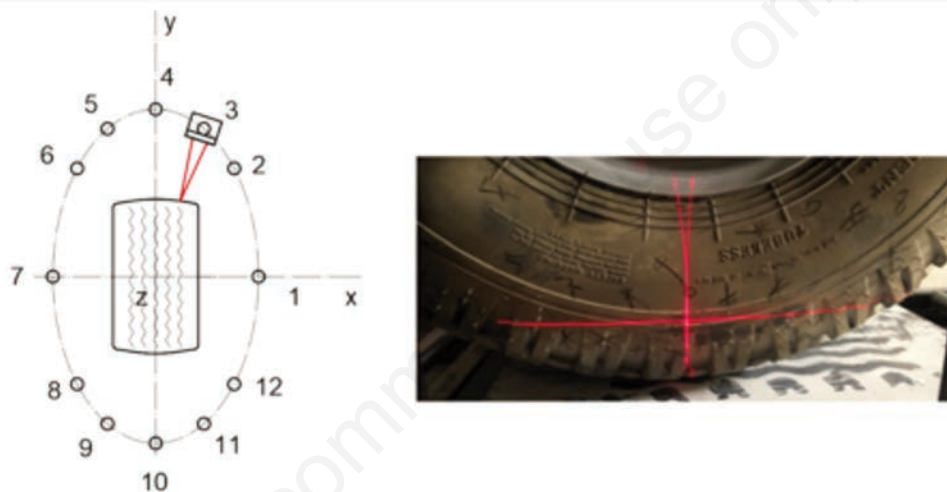


Figure 2. Positions of the scanner around the tire (left), the view of the laser beams on the scanned tire (right).



Figure 3. Tread scanning effects: the effect with scanner location points evenly spaced (left), the effect with scanner location points unevenly spaced (right).

From the horizontal section (B-B, Figure 5) it was possible to read its precise area using geometric dimensions (length, width). Then, based on the previously known vertical load value and the calculated area, it was possible to predict the contact pressure at a given rut depth. An example horizontal section made at a height corresponding to the maximum horizontal deformation of the tire is presented in Figure 6B.

It is recommended at least three repetitions for each of all combinations. The accuracy of our method is so high because the experiment is conducted in the same conditions (the same place, the same time). Therefore, in addition to the very high resolution of the scanner, the high accuracy of the whole method can be obtained. The availability of the method is dependent on the cost of the scanner - it is the most expensive element of the whole test bench. Other parts of the test bench were made from typical elements with low costs.



Figure 4. A) A spatial image of a tire profile consisting of a point cloud. B) View of the created triangle mesh prepared for cross-sectional processing (left), the effect of zooming triangle mesh (right).

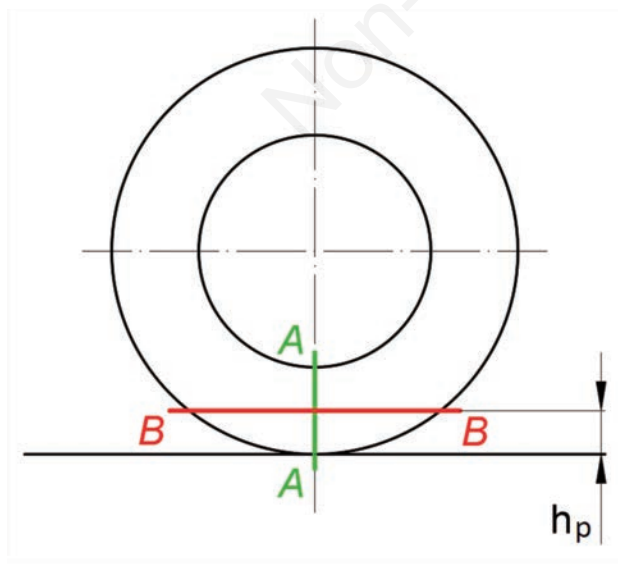


Figure 5. Location of planes making tire profile sections: A-A - vertical section plane, B-B - horizontal section plane, h_p - horizontal section plane distance from the surface.

Results

Based on the scans and cross-sections, it was possible to determine the geometrical dimensions of the widest cross-section of the tire on a plane parallel to the support plane. In the first place, the vertical deformation values were determined using vertical section analysis. A comparison of the cross-sections for the loaded and unloaded tire is presented in Figure 7A.

According to Figure 7A, at the initial load of 1275 N (resulting only from the weight of the tire and the internal frame of the test bench), the profile height was 239.6 mm, and the width was 485.0 mm. After increasing the load to 14,715 N (it was reflected the mass of 1500 kg), a flattened profile was observed, with the height lower by 25.1 mm, or about 12%. At the same time, an increase in the horizontal section area was recorded, with the width increasing by 20.2 mm (about 4%). The figure also shows the height at the greatest horizontal deformation, which amounted to 122.8 mm for the unloaded tire and 98.9 mm for the loaded tire. At these heights, horizontal sections presented in Figure 7B were subsequently drawn (in a plane parallel to the surface).

Using geometric dimensions, it was possible to measure the area of a horizontal section, which in the later stages of the analysis allowed the calculation of the tire-surface contact pressure. For the tire with the lower load, the length of the footprint was 239.6 mm, and the cross-sectional area was 89,389.2 mm² (approx. 0.089 m²). The calculated contact pressure would be 0.014 MPa in this case

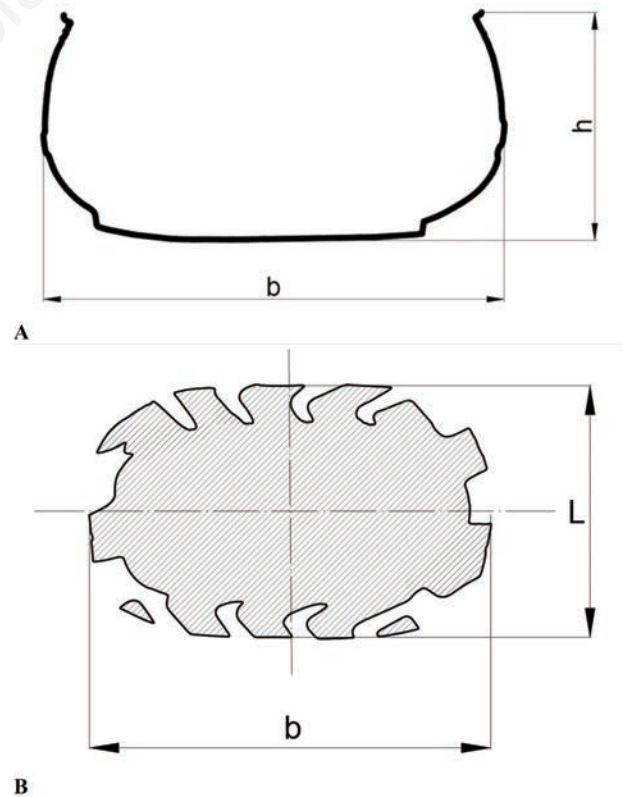


Figure 6. A) An example of a vertical section of a tire profile created in the graphics program; b - profile width (horizontal deformation), h - profile height (vertical deformation). B) An example of a horizontal section of a tire with dimensions: L - length, b - width.

(hypothesizing a sinking of the tire up to the indicated section). After increasing the load to 14,715 N, the footprint length increased by 80.1 mm (33%) and its width by 20.2 mm (4%). The cross-sectional area was 123,291.3 mm² (approx. 0.12 m²), increasing by approximately 33,902 mm² (approx. 0.03 m²), or 37.9%. With an applied load level of 14,715 N, under the same hypothesis, the contact pressure was 0.119 MPa. The significant increase in contact pressure (compared to the load of 1275 N) was mainly a result of a significant increase in vertical force. In such an experiment, it is, of course, possible to use other vertical load values in the range of up to 50,000 N, which will allow more complete studies of changes in the contact area and contact pressure.

Geometrical parameters of the tire in two different load states are presented in Figure 8. The parameter with the most significant increase due to an increase in vertical load was the length of the horizontal section - in this case, it was 32.9%. Its width increased by about 4% and the profile height by just over 14%.

Figure 9 presents the tire-surface contact area and contact pressure for two different load values. According to the graph, an increase in vertical load from 1275 to 14,715 N resulted in an increase in the contact area by 0.034 m². In addition, a significant increase in contact pressure, by 0.105 MPa, was recorded, mainly due to a significant increase in vertical load.

Discussion and conclusions

Since this is a methodological paper, it aims to present the innovative method of analysis of agricultural tires deformation. The proposed method of digital image analysis allows studying vertical and horizontal deformation of a tire with various loads and pressure applied. Thanks to the use of computer software, it was possible to measure the deflection of the tire and the area of its contact with the surface at any load applied. The data collected in the experiment can be used to study changes of such parameters in laboratory conditions without the need for time-consuming and costly field tests.

To evaluate the parameters in the tire-surface system, many methods have high accuracy (Wulfsohn and Upadhyaya, 1992; Diserens *et al.*, 2011; Taghavifar and Mardani, 2013). Unfortunately, they often allow analysing just single parameters - for example, rut depth (Diserens, 2009) or contact area (Sivarajan *et al.*, 2018; Derafshpour *et al.*, 2019). In comparison with other methods, the proposed method is complex because it can be used to quickly assess the main parameters of tire-surface systems. Because the 3D-scanning methods are becoming more popular (Farhadi *et al.*, 2018; Stawicki, 2018; Lazarević *et al.*, 2019), the presented method is rational for further use. Moreover, it can be used to evaluate deformation both the tire and soil - it will be helpful at the choice of optimal conditions of agricultural tire use.

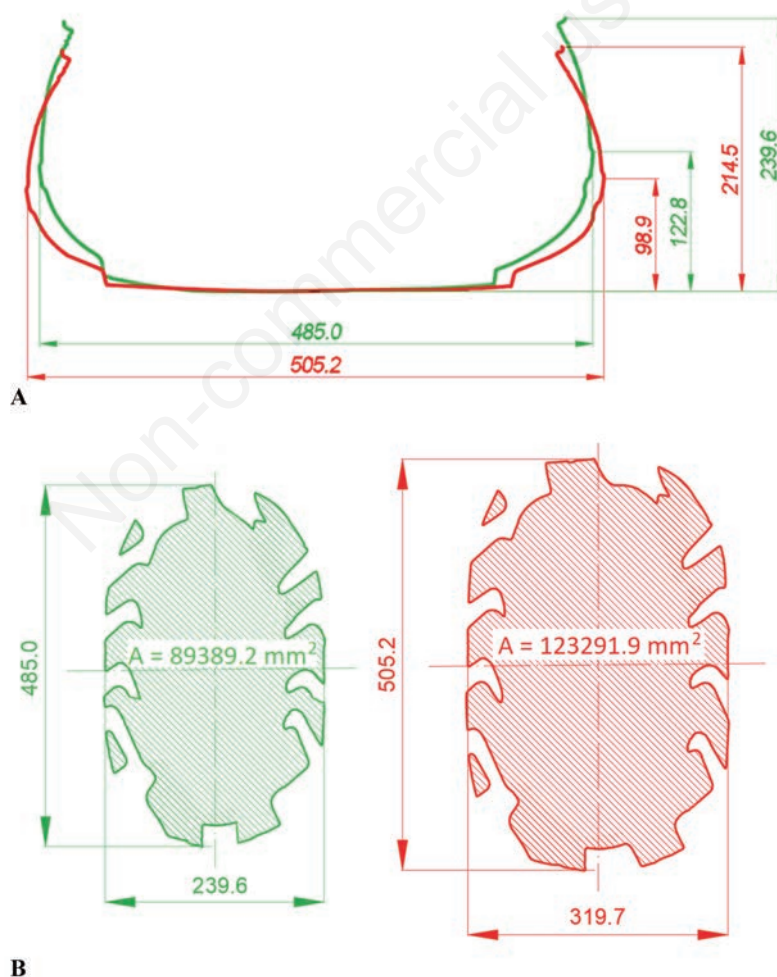


Figure 7. A) Cross-section width and height at both vertical load values: green- tire loaded with 1275 N, red- tire loaded with 14715 N. B) Horizontal sections of tire 500/50R17 profile: green- tire with 1275 N load, red- tire with 14715 N load.

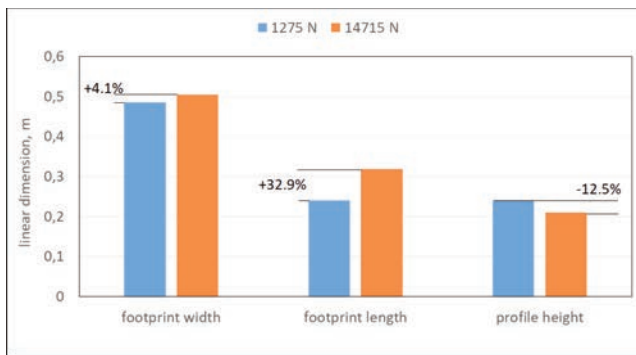


Figure 8. The effect of two vertical load levels on the width, length, and height of the tire 500/50R17 footprint and on the tire profile height at the surface-tire contact section %.



Figure 9. The tire-surface contact area and contact pressure for both vertical load values.

References

- Alontseva D.L., Ghassemieh E., Krasavin A.L., Kadyroldina A.T. 2020. Development of 3D scanning system for robotic plasma processing of medical products with complex geometries. *J. Electron. Sci. Technol.* 100057.
- Ani O.A., Uzoejinwa B.B., Ezeama A.O., Onwualu A.P., Ugwu S.N., Ohagwu C.J. 2018. Overview of soil-machine interaction studies in soil bins. *Soil Till. Res.* 175:13-27.
- Anifantis A.S., Cutini M., Bietresato M. 2020. An experimental-numerical approach for modelling the mechanical behaviour of a pneumatic tyre for agricultural machines. *Appl. Sci.* 10:3481.
- Arvidsson J., Keller T. 2007. Soil stress as affected by wheel load and tire inflation pressure. *Soil Till. Res.* 96:284-91.
- Błaszkiwicz Z. 1990. A method for the determination of the contact area between a tire and the ground. *J. Terramechan.* 27:263-82.
- Brennensthal M. 2016. Co warto wiedzieć o oponach? *AgroProfil* 6/2016.
- Da Silva Guimarães Júnnyor W., Diserens E., De Maria I.C., Junior C.F.A., Farhate C.V.V., de Souza Z.M. 2019. Prediction of soil stresses and compaction due to agricultural machines in sugarcane cultivation systems with and without crop rotation. *Sci.Total Environ.* 681:424-34.
- Derafshpour S., Valizadeh M., Mardani A., Saray M.T. 2019. A novel system developed based on image processing techniques for dynamical measurement of tire-surface contact area. *Measurement.* 139:270-6.
- Diserens E. 2009. Calculating the contact area of trailer tyres in the field. *Soil Till. Res.* 103:302-9.
- Diserens E., Défossez P., Duboisset A., Alaoui A. 2011. Prediction of the contact area of agricultural traction tires on firm soil. *Biosyst. Engine.* 110:73-82.
- Farhadi P., Golmohammadi A., Sharifi A., Shahgholi G. 2018. Potential of three-dimensional footprint mold in investigating the effect of tractor tire contact volume changes on rolling resistance. *J. Terramechan.* 78:63-72.
- Grečenko A. 1995. Tyre footprint area on hard ground computed from catalogue values. *J. Terramechan.* 32:325-33.
- Jurga J. 2008. Wpływ głębokości koleiny i ciśnienia powietrza w ogumieniu na naciski jednostkowe kół ciągników na glebę. *Inżynieria Rolnicza* 4:347-51.
- Keller T., Sandin M., Colombi T., Horn R., Or D. 2019. Historical increase in agricultural machinery weights enhanced soil stress levels and adversely affected soil functioning. *Soil Till. Res.* 194: 104293.
- Kowalski B. 2006. *Rolnictwo na kołach.* Farmer 21/2006.
- Kumar S., Pandey K.P., Kumar R., Kuma A. 2018. Effect of ballasting on performance characteristics of bias and radial ply tyres with zero sinkage. *Measurement* 121:218-24.
- Lazarević D., Nedić B., Jović S., Šarkoćević Ž., Blagojević M. 2019. Optical inspection of cutting parts by 3D scanning. *Physica A Stat. Mechan. Appl.* 121583.
- Lindemuth B.E. 2006. An overview of tire technology. *The Pneumatic Tire*, U.S. Department of Transportation, 3-7.
- Misiewicz P.A., Richards T.E., Blackburn K., Godwin R.J. 2016. Comparison of methods for estimating the carcass stiffness of agricultural tyres on hard surfaces. *Biosyst. Engine.* 147:183-92.
- Sivarajan S., Maharlooei M., Bajwa S.G., Nowatzki J. 2018. Impact of soil compaction due to wheel traffic on corn and soybean growth, development and yield. *Soil Till. Res.* 175:234-43.
- Song H.S., Sim K.S., Park T.W. 2018. Optimal tread design for agricultural lug tires determined through failure analysis. *J. Agric. Engine.* 49:64-70.
- Stawicki T. 2018. Limit wear of working parts of subsoil shanks with regard to their design solutions. *J. Res. Appl. Agric. Engine.* 63:115-20.
- Taghavifar H., Mardani A. 2013. Investigating the effect of velocity, inflation pressure, and vertical load on rolling resistance of a radial ply tire. *J. Terramechan.* 50:99-106.
- Wulfsohn D., Upadhyaya S.K. 1992. Determination of dynamic three-dimensional soil-tire contact profile. *J. Terramechan.* 29:433-64.
- Zhang J., Huang J., Fu C., Huang L., Ye H. 2020. Characterization of steel reinforcement corrosion in concrete using 3D laser scanning techniques. *Constr. Build. Mat.* 270:121402.